Journal of the Indian Society of Remote Sensing
https://doi.org/10.1007/s12524-025-02341-6

RESEARCH ARTICLE

Atmospheric Impacts of Oil Well Blowouts: A Synergistic Assessment Using Satellite Remote Sensing and WRF-Chem Modeling

Jhuma Biswas[1] · **Bijit Kumar Banerjee**[1,2,3] · **Chandrakala Bharali**[4] · **Barlin Das**[5,7] · **Binita Pathak**[5,6] · **Pradip Kumar Bhuyan**[5,6]

Received: 6 May 2025 / Accepted: 23 September 2025

Abstract

This study investigates the atmospheric impacts of the Baghjan oil well blowout in Assam, Northeast India, which occurred on 27 May 2020 and triggered a sustained fire from 9 June, lasting over five months. The incident caused significant air quality deterioration, disrupted atmospheric composition, and affected ecosystem stability. This is the first comprehensive study that combines satellite observations during the period from May 2020 to December 2020 with high-resolution WRF-Chem simulations to evaluate the atmospheric and ecological impacts of the Baghjan blowout. The analysis utilized MODIS, TROPOMI, ERA5, and IMDAA datasets, along with the WRF-Chem model (version 4.0), configured with a 30 km parent and 10 km nested domain and 33 vertical levels to simulate chemical species. This integrative approach allowed simulation of pollutant dispersion, chemical transformation, and ecosystem response. IMDAA data showed rainfall variability, with monsoon rains briefly reducing pollutants, while ERA5 wind fields revealed dominant westward and south westward dispersion. MODIS Fire Radiative Power peaked on 9 June 2020, indicating intense fire activity. NDVI and EVI values declined significantly (NDVI ~ 0.25; EVI dropped 25–30%), reflecting vegetation loss. TROPOMI data recorded increased methane levels (~ 2000 ppbv). WRF-Chem simulations captured vertical transport and episodic peaks of CH_4, PAN, ozone, and formaldehyde, suggesting active photochemistry. The presence of PAN, propylene, and propane further degraded air quality, posing health risks. Modeled near-surface methane (CH_4) concentrations peaked at 1.854 ppm, while peroxyacetyl nitrate (PAN) reached 0.920 ppm during the simulation period. On 9 June 2020, both the model simulation and TROPOMI CH_4 observations exhibited comparable surface methane concentrations, ranging approximately from 1.8 to 2.0 ppmv. The study highlights severe impacts on air quality, vegetation, and greenhouse gas emissions. It underscores the need for improved environmental monitoring, disaster preparedness, and policy intervention in environmentally sensitive regions.

Keywords WRF-Chem · FRP · PAN · GHG · MODIS · NDVI

✉ Jhuma Biswas
biswasdrjhuma@gmail.com

[1] Department of Physics, Pandu College, Guwahati 781012, Assam, India

[2] Department of Instrumentation & USIC, Gauhati University, 781014 Guwahati, India

[3] ST Radar Center, Gauhati University, Guwahati 781014, India

[4] Indian Institute of Tropical Meteorology, Pashan, Pune 411 008, India

[5] Department of Physics, Dibrugarh University, Dibrugarh 786004, India

[6] Centre for Atmospheric Studies, Dibrugarh University, Dibrugarh 786004, India

[7] Department of Physics, Jorhat Institute of Science and Technology, Jorhat 785010, Assam, India

Published online: 31 October 2025

Introduction

The complex interactions between atmospheric processes and human activities play a crucial role in driving environmental and climate changes. One significant consequence of these interactions is the occurrence of gas blowouts and oil spills, both of which pose severe environmental risks. The increasing global demand for crude oil and natural gas has raised concerns about the extraction process. One major risk is blowouts, sudden and uncontrolled releases of hydrocarbons during drilling operations. These incidents, often caused by inadequate well-control practices, human error, or unforeseen natural factors, can lead to catastrophic consequences for ecosystems and human health (Smith et al., 2021). Additionally, the discharge of produced water (PW), containing contaminants such as suspended solids, inorganic salts, soluble and non-soluble hydrocarbons, and synthetic chemicals, aggravates environmental damage, particularly to aquatic life and submerged ecosystems (Joye et al., 2011). Global records indicate that over four million onshore hydrocarbon wells have been drilled, with integrity failure rates ranging from 1.9% to 75% depending on region, well age, and design (Davies et al., 2014).

The Baghjan blowout exemplifies such well failure in the Indian context, highlighting the urgent need for stringent monitoring, maintenance, and regulatory oversight to prevent similar ecological disturbances. The total discharge of hydrocarbons during a gas blowout event is indeed critical as it directly influences the magnitude of environmental, ecological, and health consequences. Forest fires, cropland burning, and grassland combustion during a blowout release particulate matter (PM), including black carbon (BC), which contributes to atmospheric warming. Simultaneously, natural gas emissions, primarily methane (CH_4) and other hydrocarbons, significantly impact climate dynamics. Methane, a potent GHG, oxidizes in the atmosphere to form carbon dioxide (CO_2), further intensifying global warming. Multisatellite remote sensing has proven effective in quantifying methane emissions from oil and gas blowouts, as shown by the Eagle Ford Shale event, where emissions were measured ten times over a 20-day period (Cusworth et al., 2021). Higher alkanes and volatile organic compounds (VOCs) released during blowouts play a critical role in photochemical processes, such as ozone (O_3) formation. Ozone acts both as a GHG and an oxidizing agent in the atmosphere, thereby influencing the lifetimes of other GHGs, such as CH_4. The primary health risks associated with air pollution from blowouts include ozone, fine particulate matter ($PM_{2.5}$), and carcinogenic compounds such as formaldehyde, acetaldehyde, 1,3-butadiene, and benzene. The complex atmospheric reactions involving 4VOCs can also lead to the formation of secondary pollutants like peroxyacetyl nitrate (PAN). These pollutants, if released in significant quantities during blowouts, pose severe threats to human health (Garcia-Gonzales et al., 2019; Jacobson, 2019; Schade & Gregg, 2022). Recent advances in remote sensing and geospatial data science are rapidly transforming multi-disaster risk assessment and environmental monitoring. The integration of satellite data with traditional and advanced machine learning approaches has led to substantial improvements in the accuracy and scalability of land use/land cover (LULC) mapping (Alshari & Gawali, 2021), flood susceptibility modeling (Al-Ruzouq et al., 2024; Shivhare et al., 2024), and urban subsidence detection (Sudha Rani Nalakurthi et al., 2024; Thakur et al., 2025). In agriculture, remote sensing combined with ML models enables systematic crop monitoring, irrigation assessment, and rapid cyclone-induced damage mapping through customized vegetation indices and regression algorithms (Peña-Arancibia et al., 2025; Shamsuzzoha et al., 2024).

One of the most notable incidents in recent years was the gas leak at Baghjan in the state of Assam in North-East India in June, 2020. Drilled by Oil India Limited in 2006, the well produced 80,000 cubic meters of natural gas daily. On May 27, 2020, an uncontrolled release of natural gas and petroleum particles led to a catastrophic blowout while performing repairs on well no. 5, causing severe air pollution and profound impacts on both the ecosystem and local communities (Chakravartty, 2023; Colney, 2020; Talukdar, 2021). The blowout ignited on June 9, 2020, with the fire lasting over five months, destroying approximately 60–70 hectares of land around the site, displacing nearly 9000 people, and devastating 55% of the Dibru-Saikhowa landscape. The release continued for over 170 days until it was finally contained using a snubbing technique on November 15, 2020 (Baruah et al., 2024). The disaster led to severe environmental and socio-economic damage, with significant loss of biodiversity, including wetlands, grasslands, and forests, affecting both wildlife and local communities (Chakravartty, 2023). A recent study by Dutta and Kalita (2024) employed the Normalized Difference Vegetation Index (NDVI) to quantify vegetation loss due to the Baghjan blowout, highlighting the extensive ecological damage caused by the incident. During the Baghjan blowout period, total suspended matter (TSM) levels exceeded 175 kg/m^3, which is exceptionally high for a wetland ecosystem, indicating severe ecological stress on the Maguri-Motapung Wetland (Arandhara et al., 2023). A report by the Wildlife Institute of India highlighted significant health risks faced by the local population in Baghjan, particularly respiratory difficulties caused by toxic fumes released during the intense blowout period (Qureshi et al., 2020). Prolonged exposure to hazardous chemicals during and after the disaster has had lasting effects on the health of those in the region. Local news reports have documented the impact of Assam's Baghjan gas well blowout on lives, livelihoods, and the environment (Colney, 2020). Similar incidents have occurred in Assam, such as those in Dikom and Naharkatia, further underscoring the environmental and health risks posed by such events (Gogoi et al., 2007; Lahiri et al., 2016). As this industrial disaster led to the uncontrolled release of large volumes of emissions, it posed serious risks to air quality, altered atmospheric composition, and affected climate-relevant trace gases on a regional scale. These complexities make it essential to use a comprehensive atmospheric model like the Weather Research and Forecasting model coupled with Chemistry (WRF-Chem) to accurately simulate the dispersion of pollutants, their chemical transformations, and interactions with local meteorological conditions. The WRF-Chem model has been used not only to study atmospheric parameters but also to investigate monsoon-related cloud dynamics and aerosol-cloud interactions during monsoon depressions (Sarangi et al., 2015), as well as to conduct air quality forecasts (Georgiou et al., 2022). Kedia et al. (2016) showed that WRF-Chem was used to simulate aerosol and rainfall distributions over India during July 2010, and the model exhibited good agreement with both satellite and ground-based measurements. Recently, Bharali et al. (2024) reported that WRF-Chem simulated relative humidity and fog formation over the Indo-Gangetic Plains of India in good agreement with observational data. Despite the severity of the Baghjan blowout, no previous study has comprehensively analyzed its atmospheric and ecological impacts using a combined high-resolution modeling and satellite-based approach. Building on earlier approaches, this work uniquely integrates WRF-Chem simulations with multi-sensor satellite datasets to assess both atmospheric and ecological impacts of the Baghjan gas blowout in Northeast India.

In the present study, we aim to find the gas emission levels during the Baghjan gas blowout and its impact on vegetation and the environment. The meteorological conditions in the Baghjan region, which significantly influence the dispersion, transport, and deposition of pollutants is also investigated. In this study, the WRF-Chem model (Grell et al., 2005; Powers et al., 2017) is used to assess the dispersion of pollutants and hydrocarbons released during a gas blowout event, analysing the height-time intensity of CH_4, Peroxyacetyl nitrate (PAN), C_3H_8, C_3H_6, O_3, HCHO and Benzene over the affected area. Furthermore, satellite data are used to explore the changes in vegetation cover and to determine the extent of environmental degradation over time. This approach provides a detailed understanding of the blowout's impacts on the local ecosystem and air quality over Baghjan. This is the first study to integrate WRF-Chem simulations with MODIS (Moderate Resolution Imaging Spectroradiometer), TROPOMI (Tropospheric Monitoring Instrument), ERA5 (Fifth generation ECMWF atmospheric reanalysis), and IMDAA (Indian Monsoon Data Assimilation and Analysis) datasets to assess both chemical dispersion and ecological response following a gas well blowout in Northeast India.

Materials and Methods

This study employs a comprehensive methodological approach combining satellite remote sensing, meteorological reanalysis, and chemical transport modeling to evaluate the environmental consequences of the 2020 Baghjan gas blowout. Specifically, IMDAA and ERA5 reanalysis datasets are used to examine prevailing meteorological conditions during the event. Satellite products from MODIS and TROPOMI are analyzed to assess vegetation health, fire intensity, and atmospheric methane concentrations. Additionally, WRF-Chem model simulations are conducted to investigate the dispersion and vertical transport of pollutants released during the blowout. Together, these methods provide an integrated understanding of the incident's impact on air quality, atmospheric chemistry, and local ecosystems.

Study Region: Baghjan

Baghjan, located at latitude 27.4° N and longitude 95.2° E in Northeastern India, experiences a humid climate with substantial monsoon rainfall, making it wetter than most parts of the country (Fig. 1). Geologically, it lies within the Assam-Arakan Basin, which contains hydrocarbon-rich reservoirs divided into eastern, central, and western sections by two major fault trends, supporting oil and gas extraction in the region (Arandhara et al., 2023). The region is seismically active due to the presence of major tectonic features such as the Main Boundary Thrust, Main Frontal Thrust, Mishmi Thrust, Tidding Suture, Lohit, and Naga Thrust zones (Borgohain et al., 2016). To the North, Baghjan borders Dibru-Saikhowa National Park, an ecologically sensitive area that is also part of the Indo-Burma Biodiversity Hotspot, highlighting its environmental importance. The Dibru-Saikhowa Biosphere Reserve and the Maguri-Motapung wetlands, both ecologically critical zones, are located within 2 km of the blowout site. Most local communities depend on traditional livelihoods such as agriculture, fishing, and weaving, making them particularly vulnerable to environmental disasters. According to the 2011 Census, the area's population stands at 4488 (Bhatta et al., 2016).

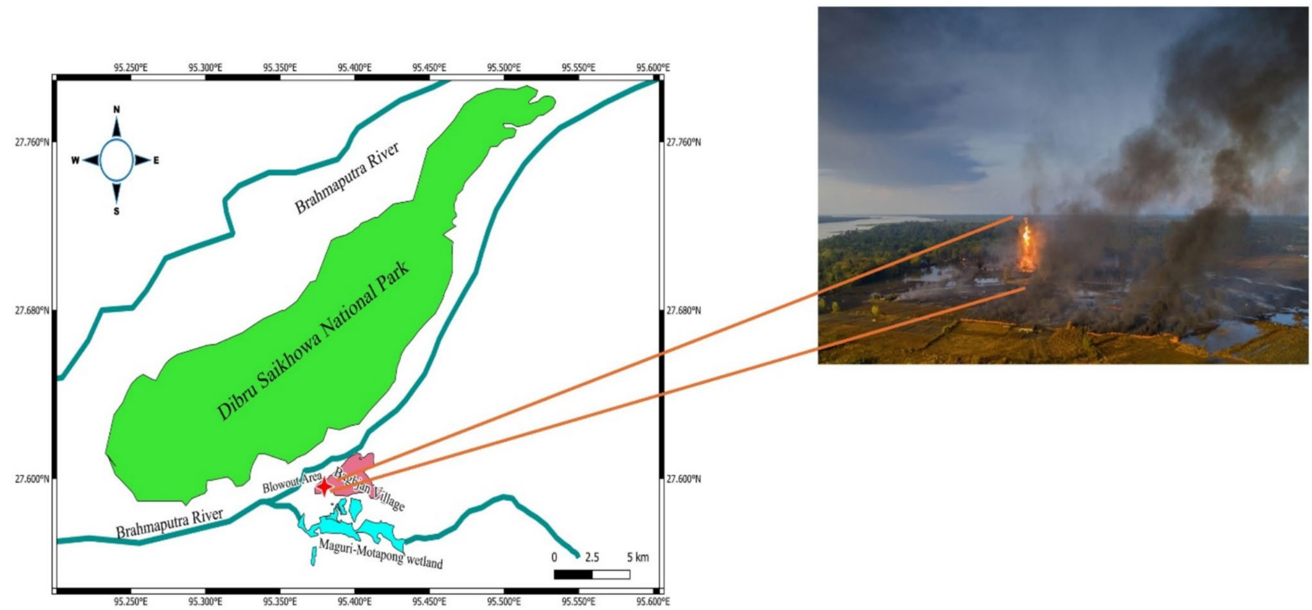

Fig. 1 Map of the study location of Baghjan showing the blowout that caught fire on 9th June 2020. Photo curtesy: Web

Meteorological Data

Indian Monsoon Data Assimilation and Analysis (IMDAA) is the first high-resolution (~12 km) regional reanalysis designed to enhance understanding of Indian monsoon variability. It captured the fine-scale features associated with a notable heavy rainfall episode over a complex terrain region (Rani et al., 2021). IMDAA reanalysis data are used to study the temporal variation of daily accumulated precipitation over Baghjan in 2020. ERA5, the fifth-generation atmospheric reanalysis produced by the European Centre for Medium-Range Weather Forecasts (ECMWF), offers hourly estimates of global climate variables with enhanced accuracy and resolution. ERA5 employs advanced 4D-Var data assimilation for accurate estimates of temperature, wind, humidity, and ocean wave heights (Hersbach et al., 2020) with a 31 km resolution and hourly outputs. To generate wind roses over Baghjan, wind data from the ERA5 reanalysis for the year 2020 were used. The wind vectors were extracted from the nearest grid point to the well location at 27.6002°N, 95.4018°E, which corresponds to the site of the gas blowout.

Remote Sensing Data

The Moderate Resolution Imaging Spectroradiometer (MODIS), aboard NASA's Terra satellite since 1999, provides near-daily global data across 36 spectral bands for Earth monitoring. It produces key land products like surface reflectance, vegetation indices, land cover maps, etc. This study assessed the blowout's impact on vegetation in Baghjan using MODIS-derived NDVI and EVI from 2018 to 2022. MODIS NDVI and EVI data used in this study are 16-day composite products at 250 m spatial resolution. Only high-quality observations were retained using standard quality assurance (QA) flags to minimize cloud and atmospheric contamination. MODIS-derived NDVI and EVI data were filtered using the Collection 6 quality flags to exclude cloudy or low-quality pixels, following validated cloud detection criteria (Marchant et al., 2020). NDVI and EVI data were spatially averaged over the region 95.00°–95.99°E and 27.00°–29.99°N, and monthly time series were generated to assess vegetation dynamics before and after the blowout. MODIS Aqua daily cloud fraction data, with a resolution of 1° × 1°, were utilized for 2020 over Baghjan. The Fire Information for Resource Management System (FIRMS) distributes near real-time active fire data from the MODIS aboard the Aqua and Terra satellites. MODIS fire data classify hotspots as 0 (vegetation fire), 1 (active volcano), 2 (stationary land fire), and 3 (offshore fire) (Giglio et al., 2009; Jain et al., 2021; Saxena et al., 2021). For this study, vegetation fire radiative power from MODIS for the blowout year 2020 was investigated. Vegetation fire was selected by considering only fires flagged as type 0. Vegetation fires data with nominal to high confidence level were used for the study. Low-confidence fires which have confidence level less than 30% were eliminated from the data set (Giglio et al., 2018). FIRMS Fire Radiative Power (FRP) datasets (1 km × 1 km), were used to detect fires in Baghjan from May 2020 to December 2020. FRP values were extracted from the nearest MODIS grid point to the well location to monitor fire intensity during the incident. Cloud cover is an important factor that may normally impact the availability of atmospheric composition data over a location. MODIS Aqua daily cloud fraction data at ($1^{\circ} \times 1^{\circ}$) resolution were used for the year 2020 over Baghjan. The Copernicus, Sentinel-5P mission, with the TROPOMI instrument, provides atmospheric monitoring and has delivered Level 2 data on gases like ozone, SO_2, NO_2, CO, formaldehyde, CH_4, and aerosols since April 2018. TROPOMI measurements were filtered to exclude cloudy scenes and high aerosol content, following the quality criteria outlined by Hu et al. (2018). CH_4 column data for Baghjan (2018–2022) was obtained from the Sentinel Open Access Hub. These values were also spatially averaged over the same 95.00°–95.99°E and 27.00°–29.99°N region, and plotted as a time series to examine blowout-phase enhancements relative to previous years. CH_4 leaks are hard to detect as they are colorless and odorless, but satellite and airborne sensors have proven effective, as seen in the Aliso Canyon leak (Thompson et al., 2016). MODIS NDVI, EVI, cloud fraction, and FRP data are freely available from NASA sources, with NDVI, EVI, and cloud data accessible via the NASA Earthdata portal, and FRP data through the FIRMS portal. CH_4 column data, derived from the Sentinel-5P TROPOMI instrument, are freely accessible from the Sentinel Open Access Hub.

WRF Chem Model

Model Overview

The Weather Research and Forecasting model coupled with Chemistry (WRF-Chem) is a powerful tool for studying atmospheric processes, including the quantification of emissions and the simulation of specific events such as blowouts (Maasakkers et al., 2022). It provides users with a range of dynamic, physical, and chemical schemes, making it highly adaptable for various atmospheric studies (Grell & Freitas, 2014; Skamarock et al., 2005). WRF-Chem's chemical transport capability allows for the projection of pollutant concentrations, such as CH_4, across the simulation domain (Abdi-Oskouei et al., 2018; Barkley et al., 2017; Pandey et al., 2019). The model is capable of simulating emission, transport, mixing, and chemical alterations of trace gasses and aerosols concurrently with meteorology using different approaches for photochemistry and aerosols (Saikia et al., 2019). The WRF-Chem model combines atmospheric chemistry with weather forecasting to simulate chemical components alongside typical meteorological variables. It includes features like dry deposition, biogenic and anthropogenic emissions, and various chemical mechanisms. Additionally, it includes tracer transport and plume rise models for specific emission scenarios (Abdi-Oskouei et al., 2018; Cusworth et al., 2021; Gogoi et al., 2017).

Model Configuration

In this study, we have used the WRF-Chem (version 4.0), model at a spatial resolution of 30 km parent (10 km, nested) domain with 33 vertical levels to simulate the chemical species over Baghjan. The simulation domain is defined on the Mercator projection and is centred at 27.4°N, 95.2° E with 60×60 with parent domain 91×91 nested domain grid points in the east–west and north–south directions, respectively (Figure S1; see supplementary file). The WRF preprocessing was carried out using the WRF Preprocessing system (WPS) version 3.7.1, which generated the necessary meteorological input files using Global Forecast System Final Analysis (GFS FNL) and Goddard Earth Observing System (GEOS) datasets (http://rda.ucar.edu/datasets/ds083.2/) with a spatial resolution of 1°, available every 6 h, to provide the initial and boundary conditions for the meteorological fields. These outputs, along with CAM-Chem chemical initial and boundary conditions, were integrated into the WRF-Chem model to simulate the blowout event. The data model integration and software are depicted in Fig. 2. The model was run for a duration of 30 days from 1st-30th June, 2020, out of which the first 4 days were discarded as spin-up, and outputs from 5th-30th June 2020 were used for analysis. The 30 km parent and 10 km nested domain resolution was selected to provide sufficient spatial detail over the Baghjan region while maintaining computational efficiency. The simulation period of June 2020 was chosen to capture the blowout onset, peak fire activity. The model outputs were post-processed using the NCAR Command Language (NCL), developed by the National Center for Atmospheric Research (NCAR), for further analysis and visualization.

Biogenic emissions of trace species are calculated online using the Model of Emissions of Gases and Aerosols from Nature (MEGAN). Anthropogenic emissions are taken from the Emissions Database for Global Atmospheric Research (EDGAR) 2011. Emissions from biomass burning are provided to the model via the Fire Inventory from NCAR version-1(FINNv2.5). Parameterizations used in this model for the study are provided in Table 1. The anthropogenic emission inventory EDGAR 2011 uses a methodology combining emission factors with technology data from organisations like the Food and Agriculture Organisation (FAO) and the International Energy Agency (IEA) with activity data specific to each country like fuel consumption (Mogno & Marvin, 2022). Emissions are at $0.1° \times 0.1°$ spatial resolution using a geographical data set of spatial proxies, including locations of energy and manufacturing facilities, road networks, shipping routes, population density, and agricultural land use (Crippa et al., 2018; Muntean et al., 2018). Global landcover data such as Leaf Area Index (LAI) and Plant Functional Types (PFTs), along with emission factors,

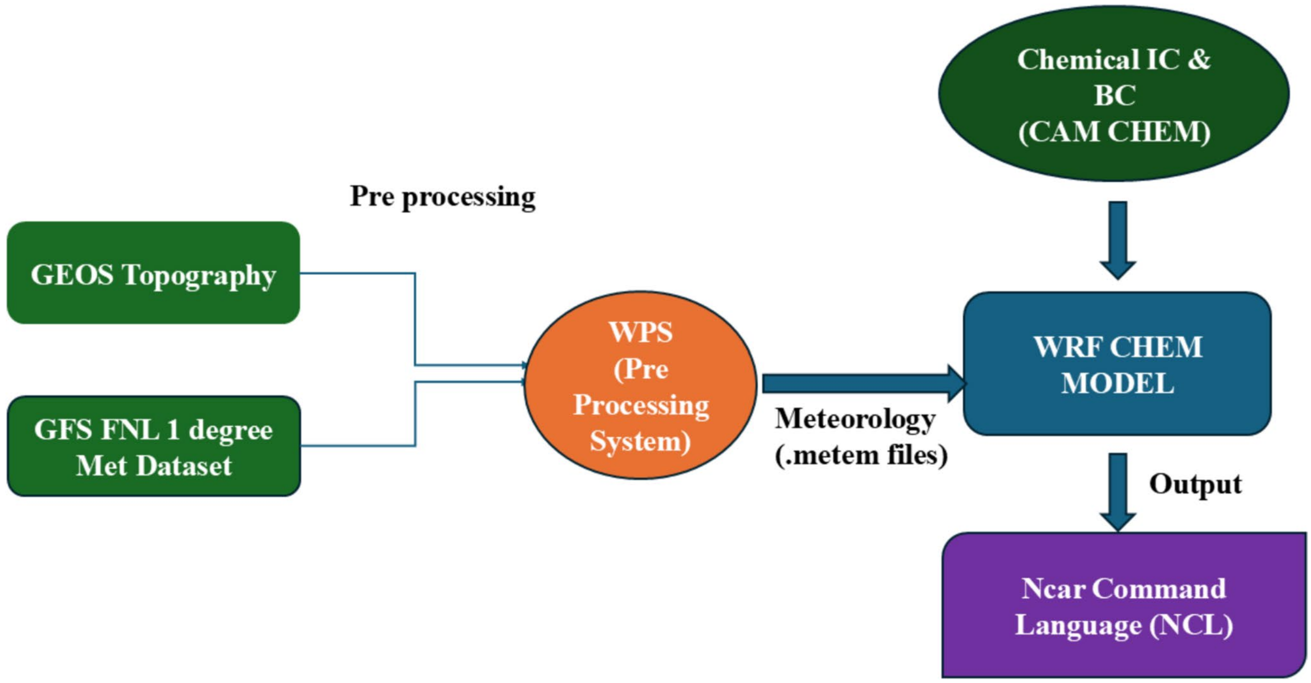

Fig. 2 Schematic of data model integration and visualization of WRF-Chem model outputs

Table 1 Configuration Parameters of WRF Chem Model

Category	Option
Chemical BC	CAM-CHEM (Buchholz et al., 2019; Emmons et al., 2020)
Meteorology BC	NCEP FNL
Physics	
Microphysics	Morrison 2–moment Scheme (Morrison et al., 2009)
Cumulus	Grell 3D Ensemble Scheme(Grell & Freitas, 2014)
PBL	Yonsei University Scheme (YSU) (Hong et al., 2006)
Land Surface	Unified Noah Land Surface Model (Tewari et al., 2004)
Longwave Physics	RRTM Longwave Scheme (Mlawer et al., 1997)
Shortwave Physics	Dudhia Shortwave Scheme (Dudhia, 1989)
Photolysis Madronich Fast-Ultraviolet–Visible Model (F-TUV)	Madronich fast-Ultraviolet–Visible Model (Madronich & Weller, 1990)
Sf_sfclay_physics	Revised MM5 scheme (Jiménez et al., 2012)
Chemistry	
Chem_opt	MOZART (Emmons et al., 2010)
Anthropogenic emissions	EDGAR 2011 (Mogno & Marvin, 2022)
Biogenic Emission	MEGAN v2.04 (Guenther et al., 2006)
Fire emissions	FINN 2.5 (Wiedinmyer et al., 2023)
Aerosol scheme	MOSAIC (Zaveri et al., 2008)

are used by MEGAN v2.04's biogenic emission inventory, combined with meteorological inputs such as temperature and solar radiation from Meteorology-Chemistry Interface Processor MCIP-processed models such as WRF. As detailed in the MEGAN documentation (Guenther et al., 2006, 2012) and in updated user guides, these inputs drive estimates for biogenic volatile organic compound emissions spatially and temporally. FINN 2.5 (Fire Inventory from NCAR version 2.5), on the other hand, calculates the fire emission inventory. FINN 2.5 uses satellite detections of active fires from MODIS as well as VIIRS sensors so as to detect smaller fires (Wiedinmyer et al., 2023).

Results and Discussion

Prevailing Meteorology

Daily accumulated precipitation over Baghjan in 2020 was estimated using IMDAA reanalysis data. The temporal variation of daily accumulated precipitation over Baghjan for the year 2020, as shown in Fig. 3, reveals significant fluctuations in rainfall throughout the study period. Located in Northeast India, Baghjan experiences substantial rainfall, which likely contributed to the initial suppression of pollutants after the blowout, which occurred during the peak monsoon season. During the pre-event phase, rainfall remained relatively low, with irregular moderate precipitation events. Around 133 mm of rainfall was recorded on the

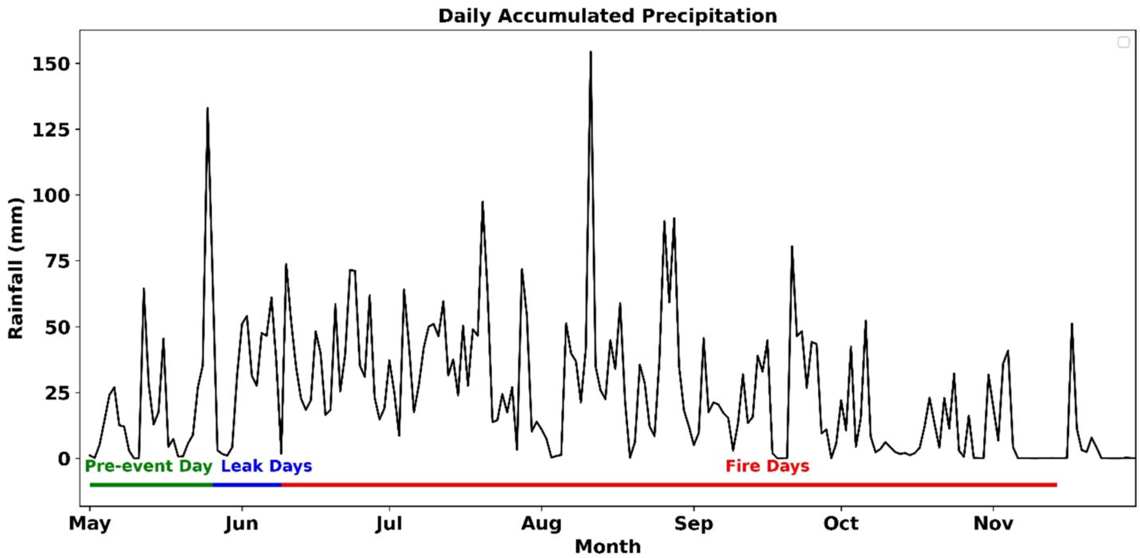

Fig. 3 Temporal variation of daily accumulated precipitation over Baghjan for the year 2020

early leak days of the event. However, during the leak days, an increase in rainfall intensity was observed, which may have influenced the dispersion of released gas and associated pollutants. Following the onset of the fire days, rainfall events became more frequent and intense, with peak precipitation exceeding 154.39 mm on 11th August 2020. The monsoon season (June–September) experienced sustained high rainfall, potentially contributing to the washout of airborne pollutants. Post-monsoon months (October–November) exhibited a gradual decline in precipitation, indicating a transition to drier conditions. These temporal variations suggest that rainfall played a crucial role in modulating the environmental impacts of the incident. Wind data from ERA5 reanalysis was used to generate wind roses, analysing wind direction statistics for different periods: The entire year 2020, Pre-event days, Leak days and fire days (Fig. 4). These wind roses, constructed from 10 m surface wind data, indicate that pollutants primarily dispersed westward and south-westward. A noticeable shift in wind direction towards the southwest (SW) and west (W) was observed during the leak days. The wind speeds were slightly stronger, which played a role in the transport of pollutants westward. The wind direction during fire days remained largely similar to the leak days, favouring westward transport. During this period, nearly 40% of the winds originated from the south, reinforcing the westward dispersion of gas. Over the year, around 19% of winds flowed from the southwest to the west, suggesting a dominant wind-driven pollutant transport in this direction. However, during the leak and fire days, the regions situated to the north and south of Baghjan experienced notably low wind speeds, leading to limited atmospheric dispersion and a deeper accumulation of pollutants in those areas (Goyal & Rama Krishna, 2002; Levy et al., 2009).

Fire During the Oil Well Blowout

The monthly fire radiative powers (FRP) obtained from MODIS are plotted (Fig. 5) from May 2020 to December 2020, covering the entire northeast India. The Baghjan fire, marked by a circle in Fig. 5, was absent before the event but became visible afterward. In May 2020, FRP values were relatively low, with scattered fire occurrences in the region. However, in June 2020, a significant rise in FRP was observed near Baghjan, marking the onset of the fire event, with radiative power reaching its peak intensity on 9th June, when the leak caught fire. In the subsequent months, FRP values declined, with only sporadic fire detections, indicating a reduction in fire intensity. Thus, higher values of FRP observed in June 2020 decreased till November and disappeared in December 2020. The fire activities in May and October-December in the other parts are common in the region due to small-scale slash burning associated with plain area cultivation (Pathak et al., 2010, 2013). The temporal variation of FRP and cloud cover over Baghjan from May to November 2020 is shown in Fig. 6, which reveals distinct patterns of fire activity and atmospheric conditions. The cloud fraction (black line) remains consistently high (close to 1) during most of the observation period, signifying persistent cloud cover. However, periodic drops in cloud fraction coincide with increased FRP values, indicating that fire activity is more detectable during clear sky conditions. The FRP is not detectable when the cloud fraction is higher, which is a discrepancy in satellite retrievals. The FRP (red bars) shows significant peaks during June and July,

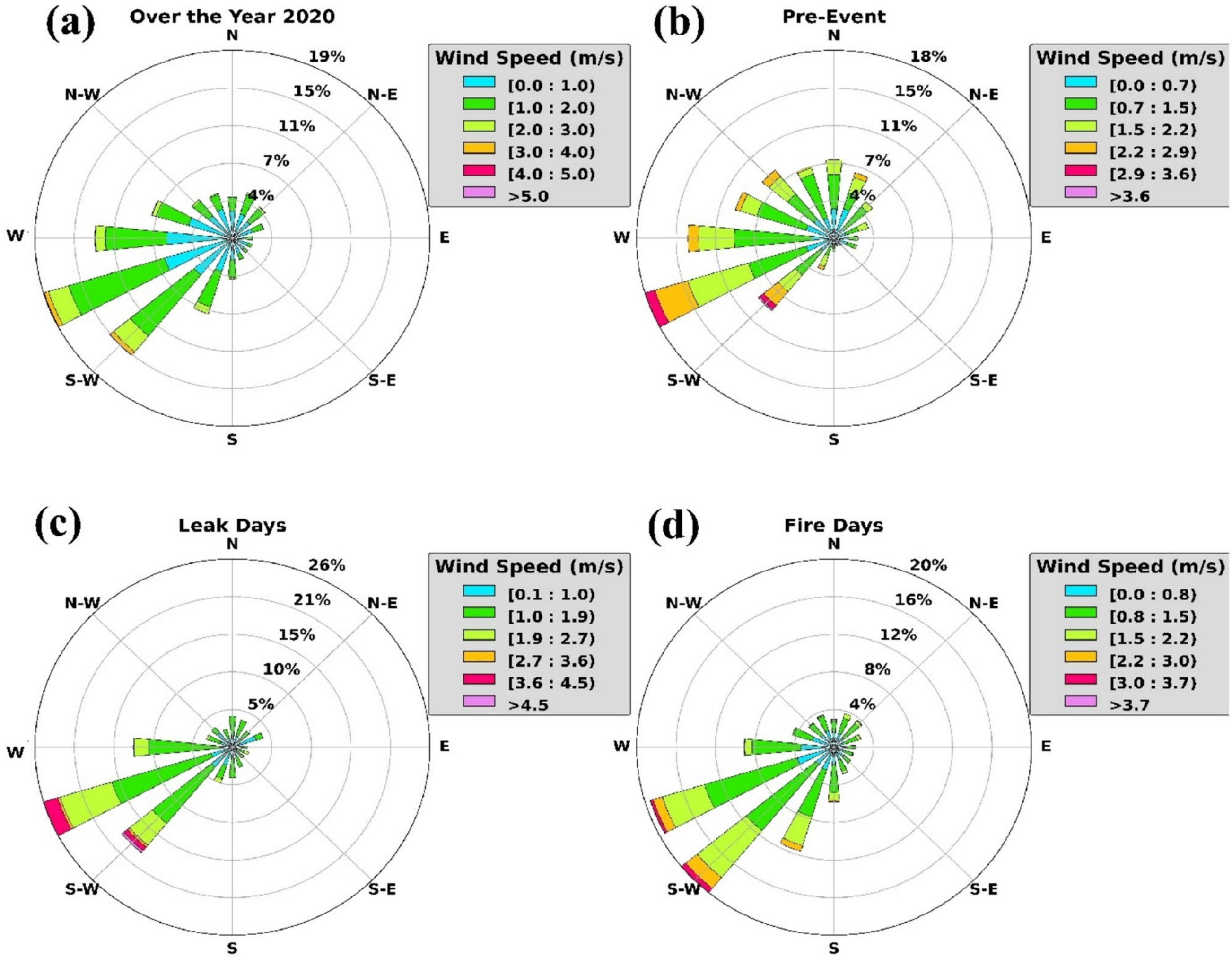

Fig. 4 Wind rose plot of 10 m surface wind speed over Baghjan

corresponding to the initial phases of the fire event. A subsequent decline in FRP is observed in August and September, indicating reduced fire activity. A secondary peak in FRP observed at the end of October, as seen from satellite data and supported by personal communication, was recorded during the period when the Canadian snubbing unit arrived at the Baghjan site on October 24, 2020 (Dutta & Kalita, 2024) to control the blowout.

Vegetation Changes

The Enhanced Vegetation Index (EVI) and Normalized Difference Vegetation Index (NDVI) are essential for evaluating the impact of disturbances like the Baghjan blowout on vegetation (Kodimalar et al., 2020; Sarmah et al., 2018). Figure 7 presents the spatial distribution of NDVI throughout 2020, highlighting a significant decline in NDVI values between June 25 and July 11. During this period, NDVI dropped sharply to a range of approximately 0.0–0.2, indicating substantial vegetation loss likely caused by the gas leak and subsequent fire at the well site. Figure 8 illustrates the monthly variation of EVI and NDVI for the Baghjan region over five years, from 2018 to 2022. A notable decline in NDVI values was observed in 2020, particularly during the monsoon season when the blowout and forest fire occurred, with values dropping sharply to around 0.25. This sharp decrease indicates extensive vegetation loss and possible degradation due to fire-induced disturbances. In contrast, during previous years, NDVI ranged between 0.32 and 0.36, while EVI remained between 0.48 and 0.51 in the monsoon season. There was a significant reduction in 2020 for both EVI and NDVI (by ~ 25–30%) compared to earlier years, indicating the severe impact of the disaster on vegetation dynamics (Figure S2; see supplementary file). This decline reflects the extensive damage to the local ecosystem, with substantial vegetation loss caused by the fire and gas blowout. Beyond environmental consequences, the reduction in vegetation also disrupted the region's

Fig. 5 Monthly FRP over North-East India, including Baghjan, from May 2020 to December 2020

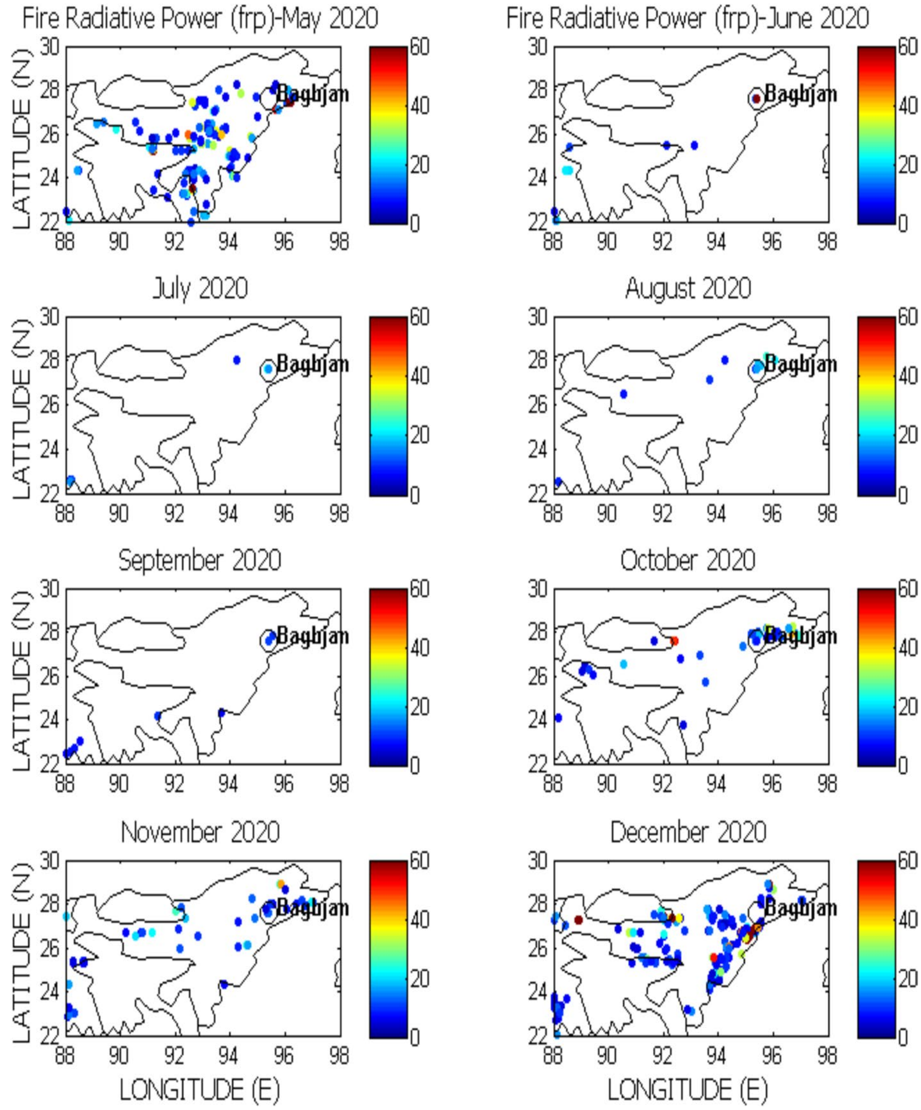

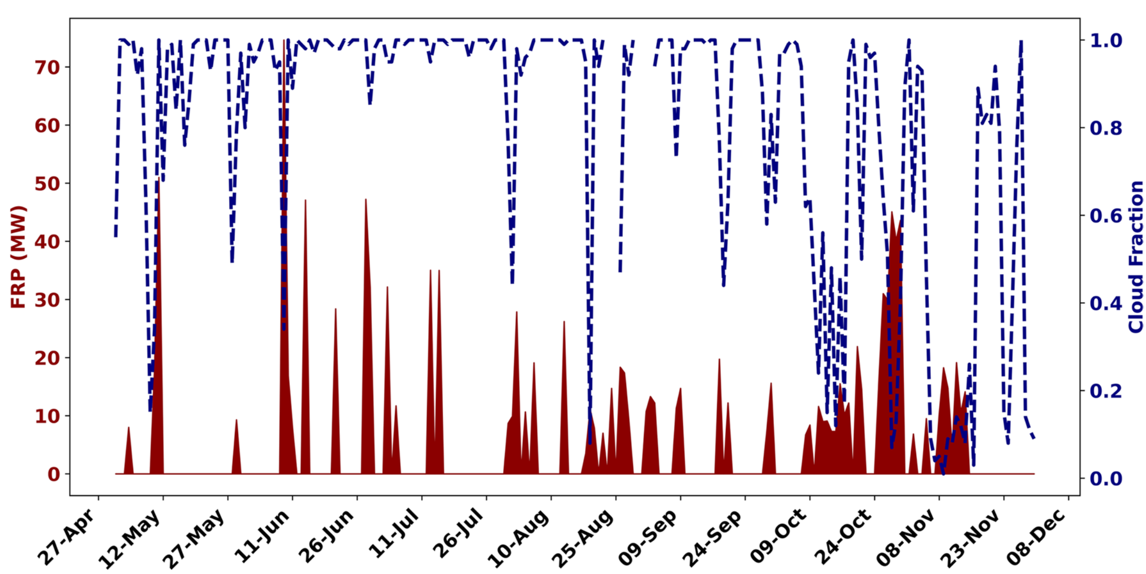

Fig. 6 Temporal variation of FRP and cloud cover represented in terms of cloud fraction over Baghjan from May to November 2020

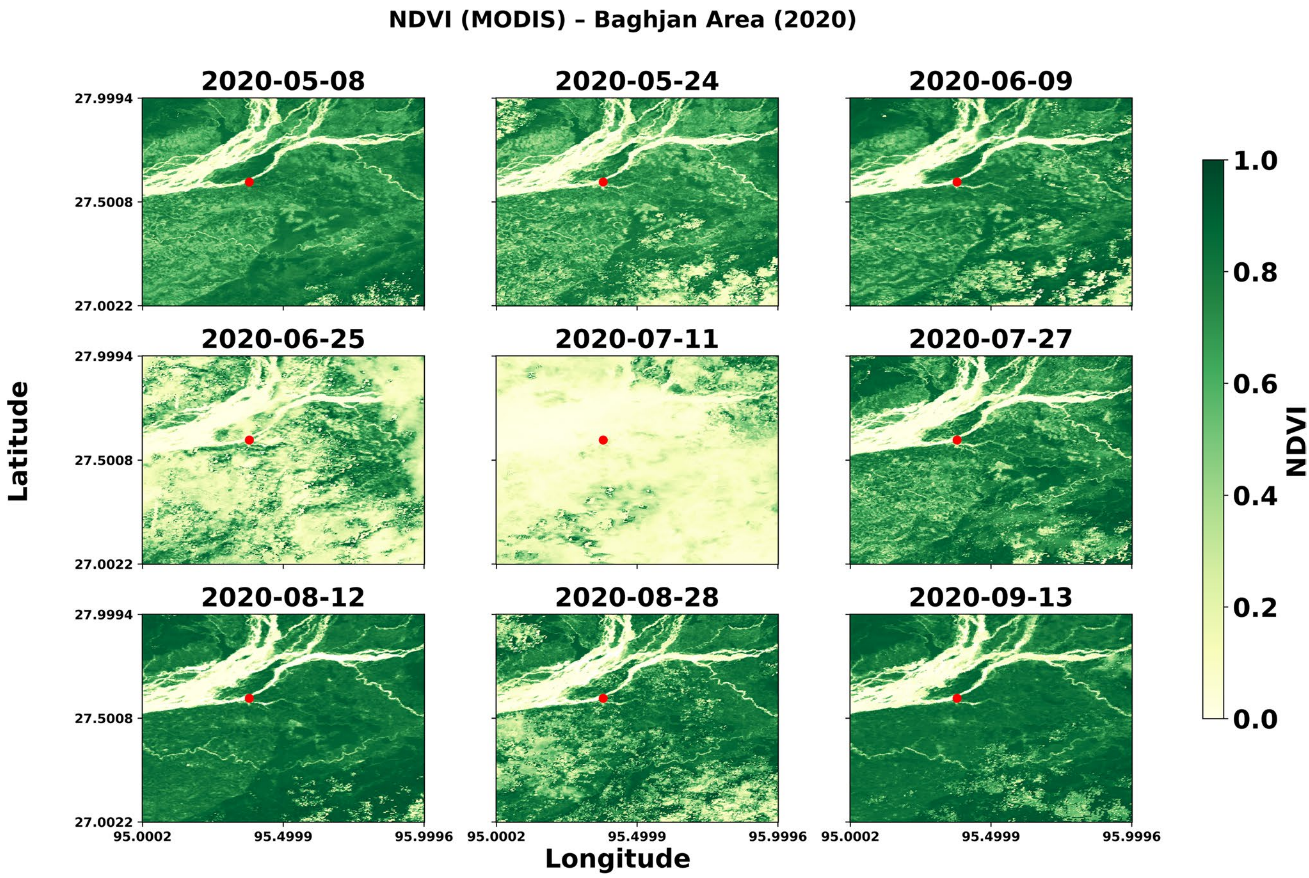

Fig. 7 Spatial variation of NDVI over the Baghjan region during 2020

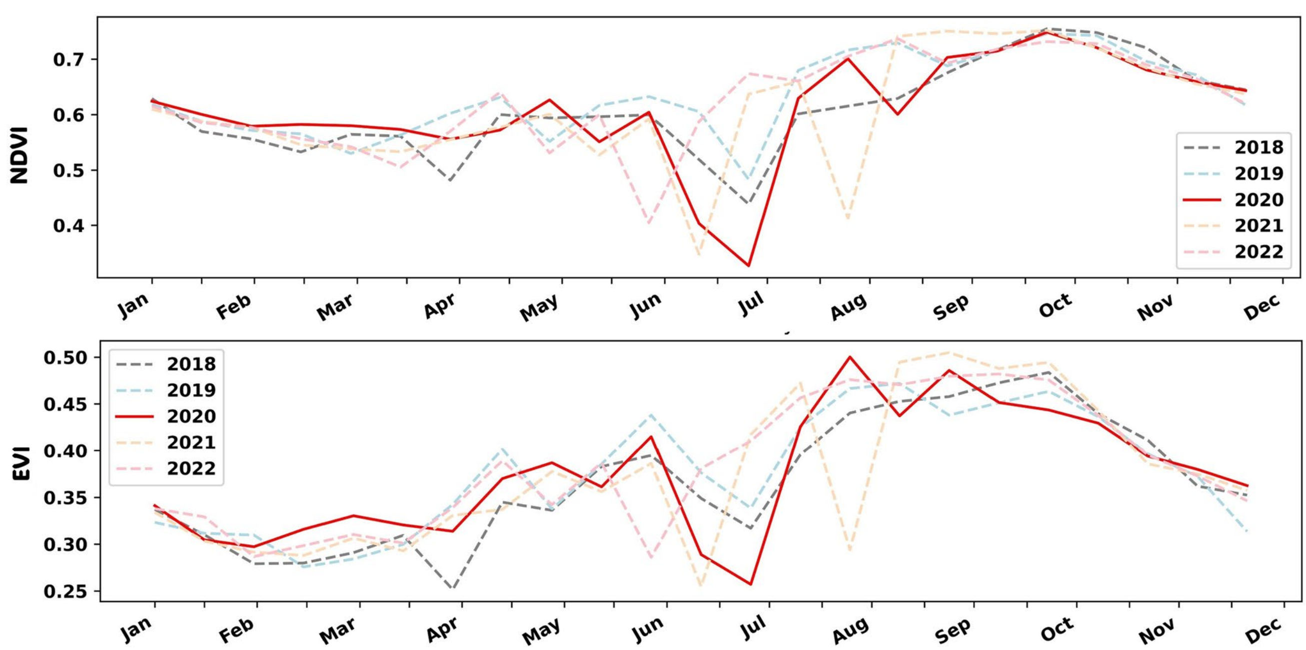

Fig. 8 Monthly variation of NDVI and EVI from 2018 to 2021 over Baghjan

economy and livelihoods, leading to crop losses and broader socio-economic instability in the affected area (Milesi et al., 2010). However, a gradual recovery is observed from August onward, suggesting post-fire regrowth and ecosystem restoration. The patterns confirm that the fire event had a temporary but substantial effect on vegetation dynamics, as captured by satellite-derived indices.

Alteration of Atmospheric Composition

Blowouts represent a significant source of global GHG emissions. Hydrocarbons like CH_4, one of the most potent GHGs, are among the major emissions released during a blowout (Cusworth et al., 2021; Maasakkers et al., 2022; Pandey et al., 2019; Schout et al., 2018). The loss at oil and gas wells, such as blowouts, can result in CH_4 emissions that are challenging to quantify from the surface. Sentinel-2 imagery, combined with a calibrated algorithm, has recently been shown to detect and quantify methane emissions from oil and gas sites (Zhang et al., 2022). Using TROPOMI data, a five-year record of CH_4 column volume mixing ratios over the blowout area has been analysed. The CH_4 levels remained relatively low during the monsoon period in 2018 and 2019, with irregular spikes. However, in 2020, a significant increase in methane concentrations was observed, with frequent high-intensity peaks, likely associated with the fire event. Irrespective of the satellite data gaps that occurred during the monsoon period, CH_4 levels of 1900–2000 ppbv were observed (Fig. 9) at the later stage of the fire period. TROPOMI CH_4 retrievals, processed through HARP (HARmonized Atmospheric Retrieval Processing), were filtered using qa_value > 0.5 (Gouw et al., 2020) to ensure reliability; under clear-sky conditions, the typical uncertainty remains within 1.5–2.5%, supporting confidence in the observed ~ 2000 ppbv peaks. Compared to previous years, a higher level of methane was detected during the gas leak period. In winter, methane contributions from crop-burning activities may overlap; however, the elevated levels detected during the fire days indicate blowout-related emissions over the study location. The spatial distribution of CH_4 concentrations during the Baghjan gas blowout event is shown in Fig. 10, which also reveals significant emissions in the affected region. Before the blowout, CH_4 concentrations were relatively low, with localized enhancements. However, post-blowout, there is a substantial increase in CH_4 levels, as indicated by the higher concentrations spreading across a wider area. The CH_4 plumes observed in the later months suggest a persistent release of gas with fluctuations in concentration and spatial coverage. The highest CH_4 levels appear in specific regions close to the blowout site, gradually dispersing over time. This trend highlights the prolonged impact of the blowout on atmospheric CH_4 levels, necessitating further assessment of its environmental and climatic implications.

Due to the unavailability of ground-based measurements from the locations of interest and also the limitation of the satellite retrievals due to the cloud contamination, it is pertinent to use a climate model to simulate the atmospheric composition at a point of spatial and temporal interest. As such, we have incorporated the WRF-Chem model to simulate hydrocarbons associated with the blowout. Figure 11 highlights the vertical profile of gases and compounds over the simulation period. Figure 11a presents the high-time-intensity (HTI) plots of methane, indicate significant vertical

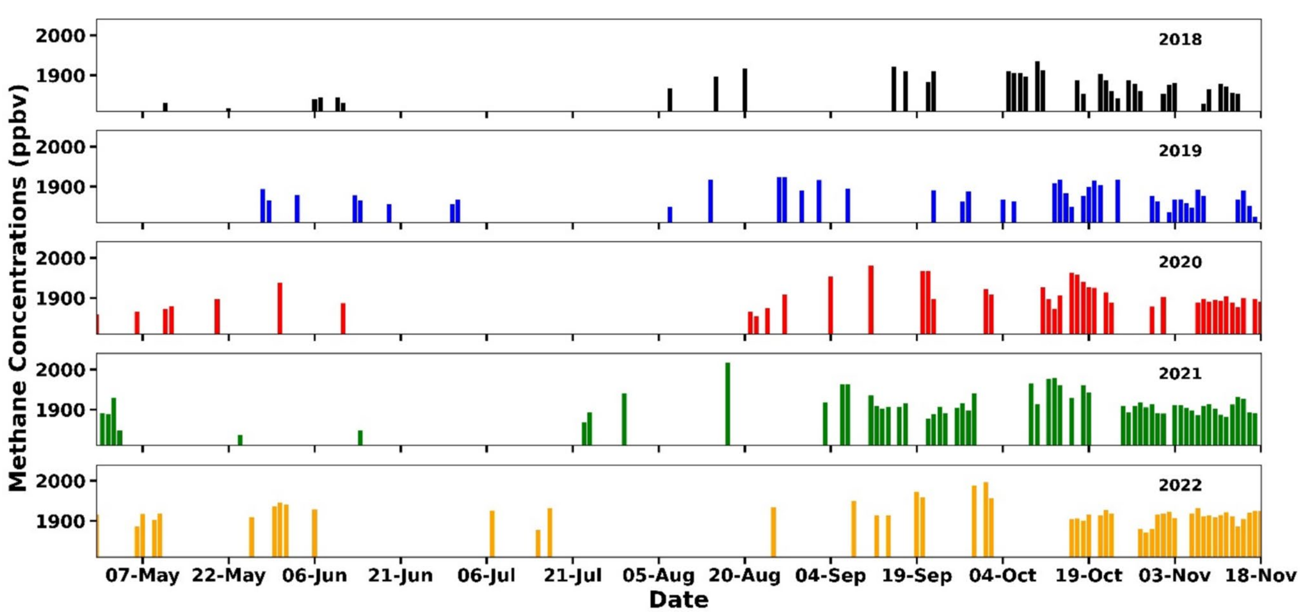

Fig. 9 Temporal variation of Methane (CH_4) concentrations from 2018 to 2022 over Baghjan

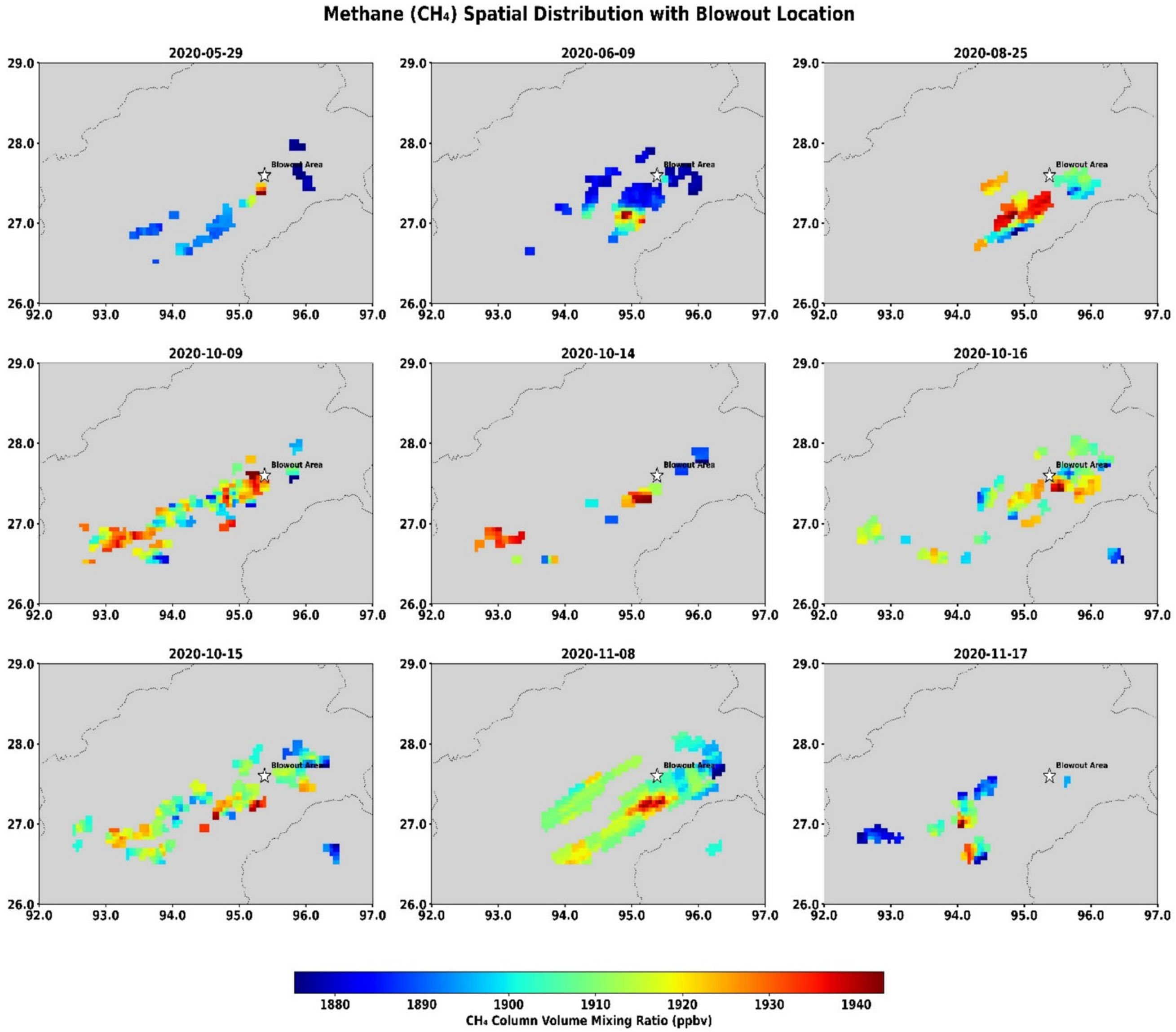

Fig. 10 The spatial distribution of methane (CH4) during the Baghjan's oil well fire event

mixing to upper atmospheric levels after the fire ignited at the well. High concentrations of CH_4 are observed near the surface, indicating strong emissions from the blowout. Limited vertical mixing suggests stable atmospheric conditions, with occasional upward transport linked to boundary layer dynamics. Notably, on 9 June 2020, when an overlap exists between the model simulation and TROPOMI CH_4 observations (Fig. 10), both show similar surface concentrations in the range of approximately 1.8 to 2.0 ppmv, affirming the consistency between modeled and satellite-detected methane levels. Similarly, the PAN time series during the event reveals a notable increase as the blowout progressed (Fig. 11). PAN forms through photochemical reactions of VOCs and NO_x, showing peaks at varying altitudes. PAN's impact on vegetation is severe (Sun & Huang, 1995) and likely contributed to the observed EVI loss during this period. Other significant hydrocarbons emitted during the blowout, as reported by the Central Pollution Control Board (CPCB) (Baruah et al., 2024), include propylene and propane. Both propylene and propane concentrations were significantly higher following the initiation of the fire (Fig. 11c, d). These VOCs remain concentrated near the surface, with propylene depleting rapidly due to its reactivity, while propane persists longer. Their episodic peaks suggest fluctuations in emissions and oxidation processes. A noticeable increase in O_3 and formaldehyde (HCHO) concentrations was observed between June 9 and June 14, 2020, as shown in Fig. 11e and f, respectively. O_3 formation is driven by NO_X and VOC, with peaks at different altitudes due to photochemical production and transport. A secondary pollutant

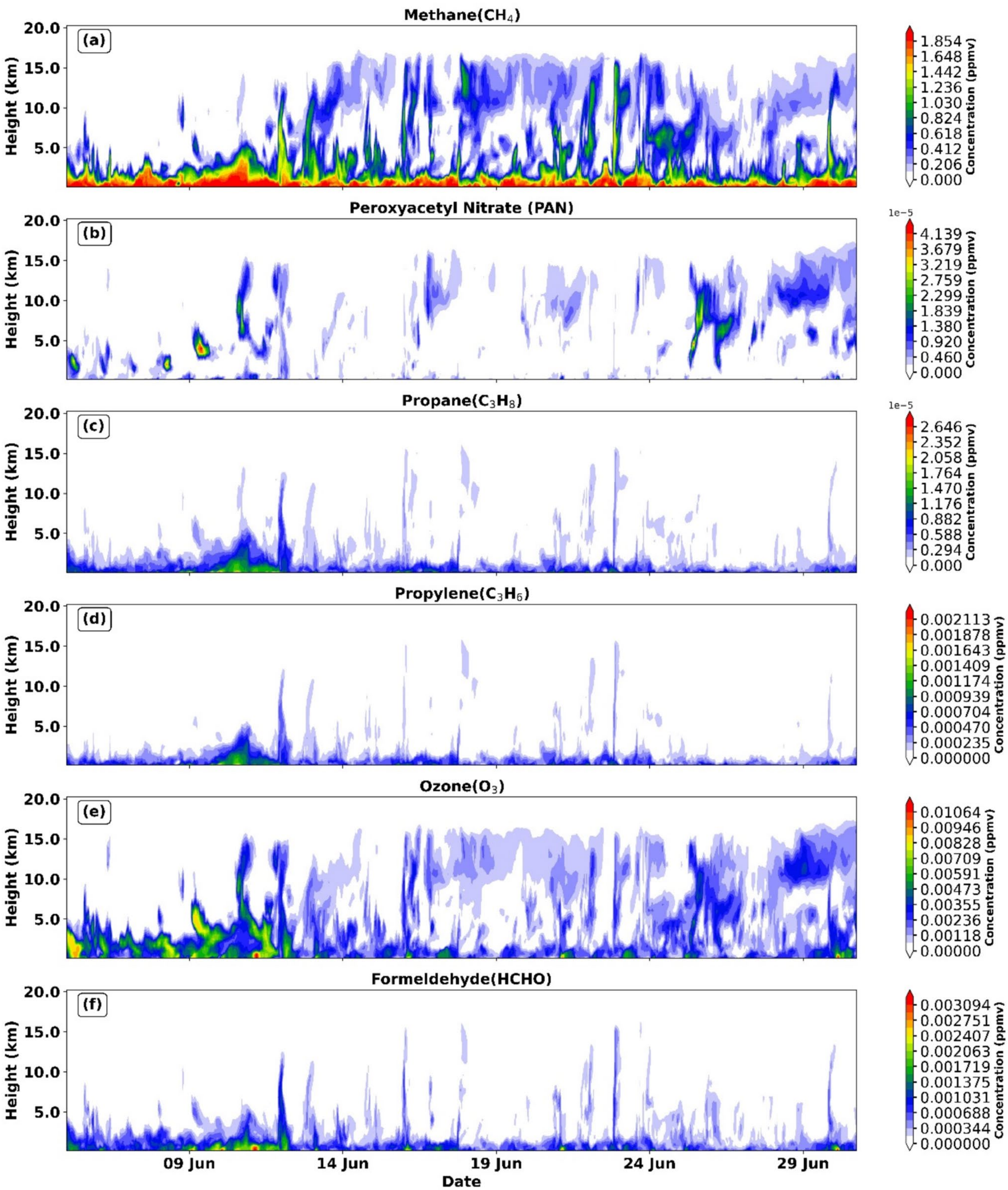

Fig. 11 WRF chem simulated **a** Methane (CH_4), **b** Peroxyacetyl nitrate (PAN), **c** Propylene(C_3H_8), **d** Propane(C_3H_6), **e** Ozone (O_3) and Formaldehyde (HCHO) over the blowout area of Baghjan

from VOC oxidation, HCHO exhibits localized peaks, indicating active photochemical processes. Its fluctuations suggest varying emission rates and reaction kinetics. It is also noted that monsoon-season variability, including frequent convection and wet deposition, may influence the accuracy of simulated pollutant dispersion and vertical transport in the WRF-Chem outputs. During this event period, both pollutants exhibited simultaneous peaks, indicating enhanced photochemical activity and secondary pollutant formation under favourable atmospheric conditions. Such elevated levels of HCHO and O_3 are of particular concern due to their combined impact on air quality and potential health risks during this time frame (Ebi & McGregor, 2008; Kim et al., 2011). These elevated levels reflect the ongoing emissions from the blowout and further highlight the severe environmental impact of the event. The increase in these hydrocarbons, alongside CH_4 and PAN, underscores the complex mixture of pollutants released during such incidents and their potential effects on air quality and vegetation. Also, the model capability of reproducing the presented chemical species is evident from the present study and is important, particularly over the complex terrain of northeast India.

Conclusions

The Baghjan blowout stands as a tragic reminder of the severe and long-lasting consequences disasters can have on the environment, the atmosphere, and local communities. Our study sheds light on the far-reaching impact of the blowout, specifically its toll on atmospheric composition, vegetation health, and regional air quality. Through satellite imagery, meteorological data, and hydrocarbon analysis, invaluable insights were obtained revealing the blowout released pollutants and subsequent fire to harm the environment. TROPOMI satellite data revealed alarming methane concentrations, peaking at 2000 ppbv during both the gas leak and the fire days. This underscores the massive contribution of the blowout to GHGs emissions. In addition to methane, the release of other hydrocarbons like propylene and propane worsened the environmental damage, showing just how complex and harmful the pollutants from such events can be. WRF-Chem simulations also revealed significant vertical transport of methane and PAN, which had a devastating effect on local vegetation, as seen in the marked decline of the region's EVI and NDVI values.

A meteorological analysis indicated that the monsoon rains initially helped to suppress the spread of pollutants, but as the fire continued into the post-monsoon season, the wind patterns shifted, pushing pollutants south-westward. The relentless fire caused widespread damage to vegetation, and the recovery of the area has been slowed down. Specifically, NDVI values declined from approximately 0.6 to as low as 0.1 during the blowout period, indicating severe vegetation stress near the well site. Additionally, both WRF-Chem simulations and TROPOMI observations showed surface methane concentrations in the range of ~ 1.8–2.0 ppmv (~ 1800–2000 ppbv) during the peak fire days, highlighting a substantial enhancement compared to background levels. However, the study is not without limitations, including retrieval gaps during the monsoon due to cloud cover, the absence of ground-based validation data, and resolution constraints in the model simulations, which should be addressed in future investigations. The findings from this study underscore the urgent need for better monitoring and response strategies to address blowout events and mitigate their environmental impact. The long-term effects on air quality, ecosystems, and the socio-economic stability of the region highlight the critical importance of swift and effective intervention. Future research should focus on ground-based validation of satellite and model outputs, long-term ecological monitoring to track recovery, and assessments of community-level health impacts to fully understand the broader consequences of such industrial disasters. The Baghjan blowout serves as a stark reminder of the risks that come with oil and gas extraction, emphasizing the need for ongoing research and stronger policies to prevent such disasters in the future.

Supplementary Information The online version contains supplementary material available at https://doi.org/10.1007/s12524-025-02341-6.

Acknowledgements This study was conducted under the Summer Research Fellowship Program 2022 (EPST15) of the Indian Academy of Sciences, received by Dr. Jhuma Biswas. BKB and BD are indebted to the Anusandhan National Research Foundation (ANRF) (formerly SERB), Government of India, for their fellowships under the SERB EMEQ and DST-SERB WEA schemes, respectively. JB is grateful to the Department of Science and Technology (DST), Government of India, for funding under the ANRF Project (EEQ/2023/001120), while BP and PKB gratefully acknowledge funding from the Indian Space Research Organization (ISRO) under the ARFI Project. The model simulations were carried out on the HPCC installed under the HICAB initiative of the DST, Government of India. BD is also grateful to the DST, Government of India, for providing him with a fellowship under the SERB WEA Project (WEA/2021/000013). The authors extend their sincere gratitude to NASA's Earthdata site, the National Centre for Medium Range Weather Forecasting (NCMRWF) portal, NASA's FIRMS portal, and the European Centre for Medium-Range Weather Forecasts (ECMWF) for providing the invaluable datasets that formed the foundation of this study. They also acknowledge the teams behind the development and operation of MODIS aboard the Terra and Aqua satellites, and TROPOMI aboard the Sentinel-5P satellite, whose cutting-edge instruments have made this research possible. Their dedication to advancing Earth observation continues to drive scientific discovery.

Author Contributions JB: Conceptualization, Data curation, Formal Analysis, Investigation, Methodology, Validation, Visualization, Writing-original draft, Writing-review and editing. BKB: Formal Analysis, Writing-original draft, Methodology, Model simulation, Visualization, Writing-review and editing. CB: Model simulation, Formal Analysis, Investigation, Validation, Visualization. BD: Model simulation, Validation, Investigation, Writing-review and editing. BP: Conceptualization, Visualization, Supervision. PKB: Conceptualization, Supervision.

Funding This research is funded by the Indian Academy of Sciences under the Summer Research Fellowship Program 2022 (EPST15), received by Dr. Jhuma Biswas, and by the Department of Science and Technology, Anusandhan National Research Foundation (ANRF) (formerly Science and Engineering Research Board), New Delhi, India, through Grant No. EEQ/2023/001120.

Declarations

Conflict of interest The authors declare that they have no conflict of interest.

References

Abdi-Oskouei, M., Pfister, G., Flocke, F., Sobhani, N., Saide, P., Fried, A., Richter, D., Weibring, P., Walega, J., & Carmichael, G. (2018). Impacts of physical parameterization on prediction of ethane concentrations for oil and gas emissions in WRF-Chem. *Atmospheric Chemistry and Physics, 18*, 16863–16883. https://doi.org/10.5194/acp-18-16863-2018

Al-Ruzouq, R., Shanableh, A., Jena, R., Gibril, M. B. A., Hammouri, N. A., & Lamghari, F. (2024). Flood susceptibility mapping using a novel integration of multi-temporal sentinel-1 data and extreme deep learning model. *Geoscience Frontiers, 15*, Article 101780. https://doi.org/10.1016/j.gsf.2024.101780

Alshari, E. A., & Gawali, B. W. (2021). Evaluation of the potentials and challenges of land observation satellites. *Global Transitions Proceedings, 2*, 73–79. https://doi.org/10.1016/j.gltp.2021.01.010

Arandhara, B., Shukla, J., & Dhyani, S. (2023). Damage assessment of Baghjan oil field blowout on terrestrial and aquatic ecosystems near Dibru Saikhowa Biosphere Reserve, Assam India. *Remote Sensing Applications: Society and Environment, 31*, Article 100999. https://doi.org/10.1016/j.rsase.2023.100999

Barkley, Z. R., Lauvaux, T., Davis, K. J., Deng, A., Miles, N. L., Richardson, S. J., Cao, Y., Sweeney, C., Karion, A., Smith, M., Kort, E. A., Schwietzke, S., Murphy, T., Cervone, G., Martins, D., & Maasakkers, J. D. (2017). Quantifying methane emissions from natural gas production in north-eastern Pennsylvania. *Atmospheric Chemistry and Physics, 17*, 13941–13966. https://doi.org/10.5194/acp-17-13941-2017

Baruah, S., Niyogi, S., Ghosh, A., Piccinini, D., Saccorotti, G., Kafka, A. L., Roth, D., Yadava, M. K., Phukan, M. K., Sastry, G. N., Abdelwahed, M. F., Kayal, J. R., Bhattacharyya, S. M., Dey, C., Gogoi, K., Chetia, T., Borthakur, P., D'Amico, S., Dutta, N., & Saikia, S. (2024). Seismic monitoring of 2020 Baghjan oil-well blowout incident in Assam. *India. Scientific Reports, 14*, 24108. https://doi.org/10.1038/s41598-024-74428-y

Bharali, C., Barth, M., Kumar, R., Ghude, S. D., Sinha, V., & Sinha, B. (2024). Role of atmospheric aerosols in severe winter fog over the Indo-Gangetic Plain of India: A case study. *Atmospheric Chemistry and Physics, 24*, 6635–6662. https://doi.org/10.5194/acp-24-6635-2024

Bhatta, L., Chaudhary, S., Pandit, A., Baral, H., Das, P., & Stork, N. (2016). Ecosystem service changes and livelihood impacts in the Maguri-Motapung Wetlands of Assam. *India. Land, 5*, 15. https://doi.org/10.3390/land5020015

Borgohain, S., Das, J., Saraf, A. K., Singh, G., & Baral, S. S. (2016). Morphodynamic changes of Lohit River, NE India: Gis-based study. *Current Science, 110*, 1810–1816.

Buchholz, R. R., Emmons, L. K., Tilmes, S., & The CESM2 Development Team (2019). CESM2.1/*CAM-chem instantaneous output for boundary conditions.* UCAR/NCAR - atmospheric chemistry observations and modeling laboratory. Subset used† Lat: 23 to 32, Lon: 99 to 99, Accessed 1 June, 2020 – 30 June, 2020, https://doi.org/10.5065/NMP7-EP60.

Chakravartty, A. (2023). Baghjan blowout: NGT directs Assam government to pay aid to affected families, Down to Earth. https://www.downtoearth.org.in/environment/baghjan-blowout-ngt-directs-assam-government-to-pay-aid-to-affected-families-91190 (Accessed 6 Feb 2025).

Colney, K. (2020). How Assam's Baghjan gas well blowout impacted lives, livelihoods and the environment. https://caravanmagazine.in/communities/assam-gas-well-baghjan-blowout-fire (Accessed 6 Feb 2025).

Crippa, M., Guizzardi, D., Muntean, M., Schaaf, E., Dentener, F., van Aardenne, J. A., Monni, S., Doering, U., Olivier, J. G. J., Pagliari, V., & Janssens-Maenhout, G. (2018). Gridded emissions of air pollutants for the period 1970–2012 within EDGAR v4.3.2. *Earth System Science Data, 10*, 1987–2013. https://doi.org/10.5194/essd-10-1987-2018

Cusworth, D. H., Duren, R. M., Thorpe, A. K., Pandey, S., Maasakkers, J. D., Aben, I., Jervis, D., Varon, D. J., Jacob, D. J., Randles, C. A., Gautam, R., Omara, M., Schade, G. W., Dennison, P. E., Frankenberg, C., Gordon, D., Lopinto, E., & Miller, C. E. (2021). Multisatellite imaging of a gas well blowout enables quantification of total methane emissions. *Geophysical Research Letters, 48*, Article e2020GL090864. https://doi.org/10.1029/2020GL090864

Davies, R. J., Almond, S., Ward, R. S., Jackson, R. B., Adams, C., Worrall, F., Herringshaw, L. G., Gluyas, J. G., & Whitehead, M. A. (2014). Oil and gas wells and their integrity: Implications for shale and unconventional resource exploitation. *Marine and Petroleum Geology, 56*, 239–254. https://doi.org/10.1016/j.marpetgeo.2014.03.001

Dudhia, J. (1989). Numerical study of convection observed during the winter monsoon experiment using a mesoscale two-dimensional model.

Dutta, U., & Kalita, S. (2024). An analytical case study of the oil well blowout at Baghjan oil field, Assam: A human and environmental perspective. *Environmental Monitoring and Assessment, 196*, 931. https://doi.org/10.1007/s10661-024-13070-7

Ebi, K. L., & McGregor, G. (2008). Climate change, tropospheric ozone and particulate matter, and health impacts. *Environmental Health Perspectives, 116*(11), 1449–1455. https://doi.org/10.1289/ehp.11463

Emmons, L. K., Schwantes, R. H., Orlando, J. J., Tyndall, G., Kinnison, D., Lamarque, J., Marsh, D., Mills, M. J., Tilmes, S., Bardeen, C., Buchholz, R. R., Conley, A., Gettelman, A., Garcia, R., Simpson, I., Blake, D. R., Meinardi, S., & Pétron, G. (2020). The chemistry mechanism in the Community Earth System Model Version 2 (CESM2). *Journal of Advances in Modeling Earth Systems*. https://doi.org/10.1029/2019ms001882

Emmons, L. K., Walters, S., Hess, P. G., Lamarque, J.-F., Pfister, G. G., Fillmore, D., Granier, C., Guenther, A., Kinnison, D., Laepple, T., Orlando, J., Tie, X., Tyndall, G., Wiedinmyer, C., Baughcum, S. L., & Kloster, S. (2010). Description and evaluation of the Model for Ozone and Related chemical Tracers, version 4 (MOZART-4). *Geoscientific Model Development, 3*, 43–67. https://doi.org/10.5194/gmd-3-43-2010

Garcia-Gonzales, D. A., Popoola, O., Bright, V. B., Paulson, S. E., Wang, Y., Jones, R. L., & Jerrett, M. (2019). Associations among particulate matter, hazardous air pollutants and methane emissions from the Aliso Canyon natural gas storage facility during the 2015 blowout. *Environment International, 132*, Article 104855. https://doi.org/10.1016/j.envint.2019.05.049

Georgiou, G. K., Christoudias, T., Proestos, Y., Kushta, J., Pikridas, M., Sciare, J., Savvides, C., & Lelieveld, J. (2022). Evaluation of WRF-Chem model (v3.9.1.1) real-time air quality forecasts over the Eastern Mediterranean. *Geoscientific Model Development, 15*, 4129–4146. https://doi.org/10.5194/gmd-15-4129-2022

Giglio, L., Loboda, T., Roy, D. P., Quayle, B., & Justice, C. O. (2009). An active-fire based burned area mapping algorithm for the MODIS sensor. *Remote Sensing of Environment, 113*, 408–420. https://doi.org/10.1016/j.rse.2008.10.006

Giglio, L., Schroeder, W., Hall, J. V., & Justice, C. O. (2018). MODIS collection 6 active fire product user's guide revision *B*. NASA. Retrieved from https://modis-fire.umd.edu/files/MODIS_C6_Fire_User_Guide_B.pdf.

Gogoi, M. M., Babu, S. S., Moorthy, K. K., Bhuyan, P. K., Pathak, B., Subba, T., Chutia, L., Kundu, S. S., Bharali, C., Borgohain, A., Guha, A., De, B. K., Singh, B., & Chin, M. (2017). Radiative effects of absorbing aerosols over northeastern India: Observations and model simulations. *Journal of Geophysical Research: Atmospheres, 122*, 1132–1157. https://doi.org/10.1002/2016JD025592

Gogoi, M. M., Bhuyan, P. K., & Krishna Moorthy, K. (2007). Possible impact of a major oil-well fire on aerosol optical depth at Dibrugarh. *Current Science, 92*, 1047–1049.

Gouw, JAd., Veefkind, J. P., Roosenbrand, E., Dix, B., Lin, J. C., Landgraf, J., & Levelt, P. F. (2020). Daily satellite observations of methane from oil and gas production regions in the United States. *Scientific Reports, 10*, Article 1379. https://doi.org/10.1038/s41598-020-57678-4

Goyal, P., & Rama Krishna, T. V. B. P. S. (2002). Dispersion of pollutants in convective low wind: A case study of Delhi. *Atmospheric Environment, 36*, 2071–2079. https://doi.org/10.1016/S1352-2310(01)00458-7

Grell, G. A., & Freitas, S. R. (2014). A scale and aerosol aware stochastic convective parameterization for weather and air quality modeling. *Atmospheric Chemistry and Physics, 14*, 5233–5250. https://doi.org/10.5194/acp-14-5233-2014

Grell, G. A., Peckham, S. E., Schmitz, R., McKeen, S. A., Frost, G., Skamarock, W. C., & Eder, B. (2005). Fully coupled "online" chemistry within the WRF model. *Atmospheric Environment, 39*, 6957–6975. https://doi.org/10.1016/j.atmosenv.2005.04.027

Guenther, A., Karl, T., Harley, P., Wiedinmyer, C., Palmer, P. I., & Geron, C. (2006). Estimates of global terrestrial isoprene emissions using MEGAN (Model of Emissions of Gases and Aerosols from Nature). *Atmospheric Chemistry and Physics, 6*, 3181–3210. https://doi.org/10.5194/acp-6-3181-2006

Guenther, A. B., Jiang, X., Heald, C. L., Sakulyanontvittaya, T., Duhl, T., Emmons, L. K., & Wang, X. (2012). The model of emissions of gases and aerosols from nature version 2.1 (MEGAN2.1): An extended and updated framework for modeling biogenic emissions. *Geoscientific Model Development, 5*, 1471–1492. https://doi.org/10.5194/gmd-5-1471-2012

Hersbach, H., Bell, B., Berrisford, P., Hirahara, S., Horányi, A., Muñoz-Sabater, J., Nicolas, J., Peubey, C., Radu, R., Schepers, D., Simmons, A., Soci, C., Abdalla, S., Abellan, X., Balsamo, G., Bechtold, P., Biavati, G., Bidlot, J., Bonavita, M., … Thépaut, J.-N. (2020). The ERA5 global reanalysis. *Quarterly Journal of the Royal Meteorological Society, 146*, 1999–2049. https://doi.org/10.1002/qj.3803

Hong, S., Noh, Y., & Dudhia, J. (2006). A new vertical diffusion package with an explicit treatment of entrainment processes. *Monthly Weather Review, 134*(9), 2318–2341. https://doi.org/10.1175/mwr3199.1

Hu, H., Landgraf, J., Detmers, R., Borsdorff, T., Aan de Brugh, J., Aben, I., et al. (2018). Toward global mapping of methane with TROPOMI: First results and intersatellite comparison to GOSAT. *Geophysical Research Letters, 45*, 3682–3689.

Jacobson, M. Z. (2019). Short-term impacts of the Aliso Canyon natural gas blowout on weather, climate, air quality, and health in California and Los Angeles. *Environmental Science & Technology, 53*, 6081–6093. https://doi.org/10.1021/acs.est.9b01495

Jain, M., Saxena, P., Sharma, S., & Sonwani, S. (2021). Investigation of forest fire activity changes over the Central India domain using satellite observations during 2001–2020. *GeoHealth, 5*, Article e2021GH000528. https://doi.org/10.1029/2021GH000528

Jiménez, P. A., Dudhia, J., González-Rouco, J. F., Navarro, J., Montávez, J. P., & García-Bustamante, E. (2012). A revised scheme for the WRF surface layer formulation. *Monthly Weather Review, 140*(3), 898–918. https://doi.org/10.1175/MWR-D-11-00056.1

Joye, S. B., MacDonald, I. R., Leifer, I., & Asper, V. (2011). Magnitude and oxidation potential of hydrocarbon gases released from the BP oil well blowout. *Nature Geoscience, 4*, 160–164. https://doi.org/10.1038/ngeo1067

Kedia, S., Cherian, R., Islam, S., Das, S. K., & Kaginalkar, A. (2016). Regional simulation of aerosol radiative effects and their influence on rainfall over India using WRFChem model. *Atmospheric Research, 182*, 232–242. https://doi.org/10.1016/j.atmosres.2016.07.008

Kim, K.-H., Jahan, S. A., & Lee, J.-T. (2011). Exposure to formaldehyde and its potential human health hazards. *Journal of Environmental Science and Health, Part C, 29*, 277–299. https://doi.org/10.1080/10590501.2011.629972

Kodimalar, T., Vidhya, R., & Eswar, R. (2020). Land surface emissivity retrieval from multiple vegetation indices: A comparative study over India. *Remote Sensing Letters, 11*, 176–185. https://doi.org/10.1080/2150704X.2019.1692384

Lahiri, S. K., Chutia, M., Gogoi, A., & Borgohain, H. (2016). Gas leakage from palaeogene reservoir in Assam–a geophysical puzzle. *Current Science*. https://doi.org/10.18520/cs/v111/i7/1242-1246

Levy, I., Mahrer, Y., & Dayan, U. (2009). Coastal and synoptic recirculation affecting air pollutants dispersion: A numerical study. *Atmospheric Environment, 43*, 1991–1999. https://doi.org/10.1016/j.atmosenv.2009.01.017

Maasakkers, J. D., Omara, M., Gautam, R., Lorente, A., Pandey, S., Tol, P., Borsdorff, T., Houweling, S., & Aben, I. (2022). Reconstructing and quantifying methane emissions from the full duration of a 38-day natural gas well blowout using space-based observations. *Remote Sensing of Environment, 270*, Article 112755. https://doi.org/10.1016/j.rse.2021.112755

Madronich, S., & Weller, G. (1990). Numerical integration errors in calculated tropospheric photodissociation rate coefficients. *Journal of Atmospheric Chemistry, 10*, 289–300. https://doi.org/10.1007/BF00053864

Marchant, B., Platnick, S., Meyer, K., & Wind, G. (2020). Evaluation of the MODIS collection 6 multilayer cloud detection algorithm through comparisons with CloudSat cloud profiling radar and CALIPS CALIOP products. *Atmospheric Measurement Techniques, 13*, 3263–3275. https://doi.org/10.5194/amt-13-3263-2020

Milesi, C., Samanta, A., Hashimoto, H., Kumar, K. K., Ganguly, S., Thenkabail, P. S., Srivastava, A. N., Nemani, R. R., & Myneni, R. B. (2010). Decadal variations in NDVI and food production in India. *Remote Sensing, 2*, 758–776. https://doi.org/10.3390/rs2030758

Mlawer, E. J., Taubman, S. J., Brown, P. D., Iacono, M. J., & Clough, S. A. (1997). Radiative transfer for inhomogeneous atmospheres: RRTM, a validated correlated-k model for the longwave. *Journal* *of Geophysical Research: Atmospheres, 102*, 16663–16682. https://doi.org/10.1029/97JD00237

Mogno, C., & Marvin, M. R. (2022). EDGAR v5.0 emissions inventory speciated for the MOZART chemical mechanism . In Zenodo (CERN European Organization for Nuclear Research). https://doi.org/10.5281/zenodo.6130620.

Morrison, H., Thompson, G., & Tatarskii, V. (2009). Impact of cloud microphysics on the development of trailing stratiform precipitation in a simulated squall line: Comparison of one- and two-moment schemes. *Monthly Weather Review, 137*, 991–1007. https://doi.org/10.1175/2008MWR2556.1

Muntean, M., Janssens-Maenhout, G., Song, S., Giang, A., Selin, E. N., Zhong, H., Zhao, Y., Olivier, J. G. J., Guizzardi, D., Crippa, M., Schaaf, E., & Dentener, F. (2018). Evaluating EDGARv4.tox2 speciated mercury emissions ex-post scenarios and their impacts on modelled global and regional wet deposition patterns. *Atmospheric Environment, 184*, 56–68. https://doi.org/10.1016/j.atmosenv.2018.04.017. ISSN 1352-2310.

Pandey, S., Gautam, R., Houweling, S., Van Der Gon, H. D., Sadavarte, P., Borsdorff, T., Hasekamp, O., Landgraf, J., Tol, P., Van Kempen, T., Hoogeveen, R., Van Hees, R., Hamburg, S. P., Maasakkers, J. D., & Aben, I. (2019). Satellite observations reveal extreme methane leakage from a natural gas well blowout. *Proceedings of the National Academy of Sciences of the United States of America, 116*, 26376–26381. https://doi.org/10.1073/pnas.1908712116

Pathak, B., Bhuyan, P. K., Biswas, J., & Takemura, T. (2013). Long term climatology of particulate matter and associated microphysical and optical properties over Dibrugarh, North-East India and inter-comparison with SPRINTARS simulations. *Atmospheric Environment, 69*, 334–344. https://doi.org/10.1016/j.atmosenv.2012.12.032

Pathak, B., Kalita, G., Bhuyan, K., Bhuyan, P. K., & Moorthy, K. K. (2010). Aerosol temporal characteristics and its impact on shortwave radiative forcing at a location in the northeast of India. *Journal of Geophysical Research: Atmospheres*. https://doi.org/10.1029/2009JD013462

Peña-Arancibia, J. L., Ahmad, M. D., & Yu, Y. (2025). Remote sensing characterisation of cropping systems and their water use to assess irrigation management from field to canal command scale. *Agricultural Water Management, 311*, Article 109374. https://doi.org/10.1016/j.agwat.2025.109374

Powers, J. G., Klemp, J. B., Skamarock, W. C., Davis, C. A., Dudhia, J., Gill, D. O., Coen, J. L., Gochis, D. J., Ahmadov, R., Peckham, S. E., Grell, G. A., Michalakes, J., Trahan, S., Benjamin, S. G., Alexander, C. R., Dimego, G. J., Wang, W., Schwartz, C. S., Romine, G. S., … Duda, M. G. (2017). The weather research and forecasting model: Overview, system efforts, and future directions, B. *American Meteorological Society, 98*, 1717–1737. https://doi.org/10.1175/BAMSD-15-00308.1

Qureshi, Q., Kolipakam, V., Wakid, A., Jacob, M., Gayathri, A., & Singh, V. (2020). Impact of oil well blowout at Baghjan oil field, Assam and resulting oil spill, on surrounding landscape. Wildlife Institute of India, 1–171, https://www.indiaspend.com/wp-content/uploads/2020/09/Bhagjan-report1.pdf

Rani, S. I., Arulalan, T., George, J. P., Rajagopal, E. N., Renshaw, R., Maycock, A., Barker, D. M., & Rajeevan, M. (2021). IMDAA: high-resolution satellite-era reanalysis for the Indian Monsoon Region. *Journal of Climate, 34*, 5109–5133. https://doi.org/10.1175/JCLI-D-20-0412.1

Saikia, A., Pathak, B., Singh, P., Bhuyan, P. K., & Adhikary, B. (2019). Multi-model evaluation of meteorological drivers, air pollutants and quantification of emission sources over the Upper Brahmaputra Basin. *Atmosphere, 10*, Article 703. https://doi.org/10.3390/atmos10110703

Sarangi, C., Tripathi, S. N., Tripathi, S., & Barth, M. C. (2015). Aerosol-cloud associations over Gangetic Basin during a typical monsoon depression event using WRF-Chem simulation. *Journal of Geophysical Research: Atmospheres, 120*, 10974–10995. https://doi.org/10.1002/2015JD023634

Sarmah, S., Jia, G., Zhang, A., & Singha, M. (2018). Assessing seasonal trends and variability of vegetation growth from NDVI3g, MODIS NDVI and EVI over South Asia. *Remote Sensing Letters, 9*, 1195–1204. https://doi.org/10.1080/2150704X.2018.1519270

Saxena, P., Sonwani, S., Srivastava, A., Jain, M., Srivastava, A., Bharti, A., Rangra, D., Mongia, N., Tejan, S., & Bhardwaj, S. (2021). Impact of crop residue burning in Haryana on the air quality of Delhi, India. *Heliyon, 7*, Article e06973. https://doi.org/10.1016/j.heliyon.2021.e06973

Schade, G. W., & Gregg, M. L. (2022). Testing HYSPLIT plume dispersion model performance using regional hydrocarbon monitoring data during a gas well blowout. *Atmosphere, 13*, 486. https://doi.org/10.3390/atmos13030486

Schout, G., Hartog, N., Hassanizadeh, S. M., & Griffioen, J. (2018). Impact of an historic underground gas well blowout on the current methane chemistry in a shallow groundwater system. *Proceedings of the National Academy of Sciences of the United States of America, 115*, 296–301. https://doi.org/10.1073/pnas.1711472115

Shamsuzzoha, M., Shaw, R., & Ahamed, T. (2024). Machine learning system to assess rice crop change detection from satellite-derived RGVI due to tropical cyclones using remote sensing dataset. *Remote Sensing Applications: Society and Environment, 35*, Article 101201. https://doi.org/10.1016/j.rsase.2024.101201

Shivhare, V., Kumar, A., Kumar, R., Shashtri, S., Mallick, J., & Singh, C. K. (2024). Flood susceptibility and flood frequency modeling for lower Kosi Basin, India using AHP and Sentinel-1 SAR data in geospatial environment. *Natural Hazards, 120*, 11579–11610. https://doi.org/10.1007/s11069-024-06614-0

Skamarock, W. C., Klemp, J. B., Dudhia, J., Gill, D. O., Barker, D. M., Wang, W., & Powers, J. G. (2005). A description of the advanced research WRF version 2. National center for atmospheric research technical note TN-468 + STR, 88 (Available from NCAR, P. O. Box 3000, Boulder, CO 80307).

Smith, P. K., Craig, B. N., Wang, Q., & Larrañaga, M. D. (2021). Human error analysis of the Montara well blowout. *Process Safety Progress, 40*, Article e12182. https://doi.org/10.1002/prs.12182

Sudha Rani Nalakurthi, N. V., Behera, M. R., & Bhaskaran, P. K. (2024). Land subsidence detection using sentinel-1 interferometer and its relation with environmental drivers: A case study for coastal Mumbai city. *Spatial Information Research, 32*, 665–681. https://doi.org/10.1007/s41324-024-00588-8

Sun, E.-J., & Huang, M.-H. (1995). Detection of peroxyacetyl nitrate at phytotoxic level and its effects on vegetation in Taiwan. *Atmospheric Environment, 29*, 2899–2904. https://doi.org/10.1016/1352-2310(94)00329-J

Talukdar, S. (2021). Report on Baghjan blowout says it may take more than 10 years for even a partial recovery of the destruction caused to the landscape, Frontline. https://frontline.thehindu.com/environment/disaster-baghjan-oil-well-blowout-tinsukia-assam-2021-report/article34987694.ece.

Tewari, M., Chen, F., Wang, W., Dudhia, J., LeMone, M. A., Mitchell, K. E., Ek, M. B., Gayno, G., Wegiel, J. W., & Cuenca, R. (2004). January 14. Implementation and verification of the unified Noah land-surface model in the WRF model. 20th conference on weather analysis and forecasting/16th conference on numerical weather prediction, Seattle, US. https://opensky.ucar.edu/islandora/object/conference%3A1576.

Thakur, A. K., Garg, R. D., & Jain, K. (2025). An assessment of different line-of-sight and ground velocity distributions for a comprehensive understanding of ground deformation patterns in East Jharia coalfield. *Remote Sensing Applications: Society and Environment, 37*, Article 101446. https://doi.org/10.1016/j.rsase.2024.101446

Thompson, D. R., Thorpe, A. K., Frankenberg, C., Green, R. O., Duren, R., Guanter, L., Hollstein, A., Middleton, E., Ong, L., & Ungar, S. (2016). Space-based remote imaging spectroscopy of the Aliso Canyon CH_4 superemitter. *Geophysical Research Letters, 43*, 6571–6578. https://doi.org/10.1002/2016GL069079

Wiedinmyer, C., Kimura, Y., McDonald-Buller, E. C., Emmons, L. K., Buchholz, R. R., Tang, W., Seto, K., Joseph, M. B., Barsanti, K. C., Carlton, A. G., & Yokelson, R. (2023). The fire inventory from NCAR version 2.5: An updated global fire emissions model for climate and chemistry applications. *Geoscientific Model Development, 16*, 3873–3891. https://doi.org/10.5194/gmd-16-3873-2023

Zaveri, R. A., Easter, R. C., Fast, J. D., & Peters, L. K. (2008). Model for simulating aerosol interactions and chemistry (MOSAIC). *Journal of Geophysical Research: Atmospheres*. https://doi.org/10.1029/2007jd008782

Zhang, Z., Sherwin, E. D., Varon, D. J., & Brandt, A. R. (2022). Detecting and quantifying methane emissions from oil and gas production: Algorithm development with ground-truth calibration based on Sentinel-2 satellite imagery. *Atmospheric Measurement Techniques, 15*, 7155–7169. https://doi.org/10.5194/amt-15-7155-2022